G. Bertuccio, M. Ahangarianabhari, C. Graziani, D. Macera, Y. Shi, A. Rachevski, I. Rashevskaya, A. Vacchi, G. Zampa, N. Zampa, P. Bellutti, G. Giacomini, A. Picciotto, C. Piemonte, N. Zorzi**, X-Ray Silicon Drift Detector – CMOS Front-End System with High Energy Resolution at Room Temperature,** IEEE TRANSACTIONS ON NUCLEAR SCIENCE, Volume: 63, Issue: 1, Feb. 2016, pp. 400-406, DOI: 10.1109/TNS.2015.2513602

X-Ray Silicon Drift Detector – CMOS Front-End System with High Energy Resolution at Room Temperature

G. Bertuccio, M. Ahangarianabhari, C. Graziani, D. Macera, Y. Shi, A. Rachevski, I. Rashevskaya,
A. Vacchi, G. Zampa, N. Zampa, P. Bellutti, G. Giacomini, A. Picciotto, C. Piemonte, N. Zorzi

***Abstract*— We present a spectroscopic system constituted by a Silicon Drift Detector (SDD) coupled to a CMOS charge sensitive preamplifier, named SIRIO, specifically designed to reach ultimate low noise levels. The SDD, with an active area of 13 mm^2, has been manufactured by optimizing the production processes in order to reduce the anode current, successfully reaching current densities between 17 and 25 pA/cm^2 at +20°C for drift fields ranging from 100 to 500 V/cm. The preamplifier shows minimum intrinsic noise levels of 1.27 and 1.0 electrons r.m.s. at +20°C and -30°C, respectively. At room temperature (+20°C) the ^{55}Fe 5.9 keV and the pulser lines have 136 eV and 64 eV FWHM, respectively, corresponding to an equivalent noise charge of 7.4 electrons; the noise threshold is at 165 eV. The energy resolution, as measured on the pulser line, ranges from 82 eV FWHM (9.4 electrons r.m.s.) at +30°C down to 29 eV FWHM (3.3 electrons r.m.s.) at -30°C.**

***Index Terms*— Semiconductor radiation detectors, Silicon radiation detectors, Semiconductor Drift Detectors, X-ray detectors, room temperature detectors, X-ray spectroscopy, application specific integrated circuits, CMOS integrated circuits, Low-noise amplifiers, Charge Sensitive Preamplifiers.**

I. INTRODUCTION

A. Semiconductor Drift Detectors

SEMICONDUCTOR Drift Detectors (SDDs) were invented by E. Gatti and P. Rehak in 1983 [1, 2] and suddenly opened new perspectives in radiation and particle detection and spectroscopy because of the higher energy resolution achievable with respect to traditional junction diodes. Figure 1(a) shows a cross section of a cylindrical-type SDD: the p+ cathodes are biased to fully deplete the silicon bulk and to generate an electrostatic potential energy for the electrons - in Figure 1(b) - whose minimum stays at a small n+ electrode (anode) usually placed at the center of the device. The electrons generated by the radiation are so driven toward the anode and collected there. The SDD's anode capacitance is extremely low (≈ 0.1 pF) - because of its small geometrical dimension and of the fully depleted semiconductor - and independent from the detector active area. Therefore, SDDs can be designed with large sensitive area (up to several cm^2) but with the output capacitance of a small pixel. Differently, a traditional semiconductor detector based on planar Schottky or pn junction has a capacitance directly proportional to the junction area with a specific capacitance of about 34 pF/cm^2 for a 300 µm thick detector. Since the noise of a detection system based on a junction semiconductor detector significantly decreases by lowering the capacitance of the detector output electrode, SDDs have brought a breakthrough with respect to traditional detectors for which a tradeoff between large sensitive area, low noise and number of readout channels were strictly necessary. In addition, the very small capacitance of the SDD anode not only reduces the contribution of system series noise but also shortens the optimum shaping time τ_{opt} so that the contribution of the parallel white noise - arising from the detector current - is reduced as well. Besides, SDDs allow also low noise operation at high photon/particle rate because of the shorter τ_{opt}.

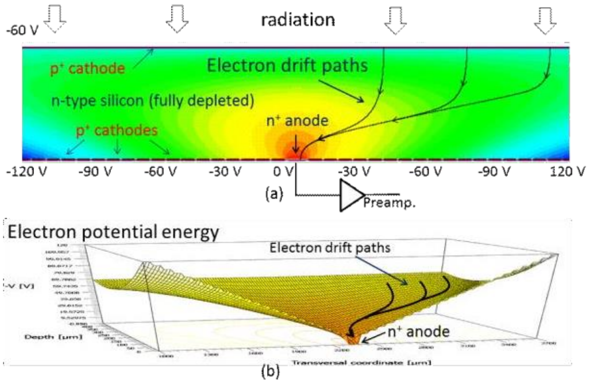

Figure 1 (a) Section of a cylindrical Silicon Drift Detector; (b) Potential energy of the electrons in the SDD. The electrons generated by the radiation drift toward the anode electrode, where the minimum potential energy is placed by means of a proper bias of a set of cathodes.

Manuscript submitted July 30, 2015.

G. Bertuccio, M. Ahangarianabhari, and Y. Shi are with Politecnico di Milano, Department of Electronics, Information and Bioengineering, Polo Territoriale di Como, Via Anzani 42, 22100 Como, Italy and with National Institute of Nuclear Physics – INFN - sez. Milano
(corresponding author: G. Bertuccio, phone: +39.031.332.7346;
e-mail: Giuseppe.Bertuccio@polimi.it).

C. Graziani, D. Macera were with Politecnico di Milano - Department of Electronics, Information and Bioengineering. They are now with ST Microelectronics Srl, Milan, Italy.

A. Vacchi is with Mathematics and Informatics Department, Udine University, Via delle Scienze 206, Udine, Italy and with the Italian National Institute for Nuclear Physics INFN, sez. Trieste, Padriciano 99, 34012 Trieste, Italy.

A. Rachevski, I. Rashevskaya, G. Zampa and N. Zampa are with the National Institute of Nuclear Physics - INFN – sez. Trieste, Padriciano, 99, 34149, Trieste, Italy

P. Bellutti, G. Giacomini, A. Picciotto, C. Piemonte and N. Zorzi are with Fondazione Bruno Kessler – FBK - Via Sommarive 18, I-38123, Trento, Italy

In the last 30 years, a worldwide research and development activity has been carried out to study and design different topologies of X-ray SDDs which nowadays are widely used in many scientific experiments as well as in several commercially available X-ray spectrometers for scientific, industrial and medical applications [3, 4].

B. The limit of the detector operating temperature

One of the limits of all the semiconductor X-ray detectors with active areas above 1 mm^2, including SDDs, is their relatively high dark current - and consequently high noise - at room temperature, so that cooling the device is strictly necessary in order to achieve a high energy resolution. This is valid also for wide bandgap compound semiconductors such as CdTe and CdZnTe for which room temperature operation is limited to spectroscopy of high energy photons (50 keV – 10 MeV) only, where energy resolutions in the keV range or even higher are adequate.

The upper limit of the operating temperature of SDDs is determined by the anode current density, which currently ranges between few nA/cm^2 down to 200 pA/cm^2 at room temperature for both typical and state of the art detectors [17]. Practically, SDDs for X-ray spectroscopy operate at temperatures between -20°C and -55°C in order to reduce the anode current down to tens of fA, so reaching the highest energy resolution.

C. The SDD Front-End Electronics

The Front-End Electronics (FEE) is a fundamental part of an X-ray spectroscopic system; its importance in achieving the ultimate performance from the system is as high as the detector quality. Although Junction Field Effect Transistors (JFETs) are able to guarantee high performance due to their ultra low *1/f* noise, the very low capacitance of SDDs allows using also MOSFETs input integrated circuit preamplifiers because their size scalability permits a much better capacitive matching with the detector. In 1997 Rehak et al. proved this solution with excellent results [5]. Further research have brought to CMOS Charge Sensitive Preamplifiers with few electrons noise [6] and, some year later, this has been applied to SDDs readout as an alternative to JFETs [7].

D. Motivation and objective of this work

High resolution X-ray spectroscopy in the 0.1-20 keV energy range with the system operating at room temperature is appealing because of the advantage of avoiding cooling systems, which are relatively bulky, heavy, with power consumption in the Watt range and requires vacuum or sealed dry enclosures. SDDs are the most promising candidate to achieve this goal and have been tested at room temperature from 1992 to present. Some progress has been done in term of energy resolution and larger active area, as shown in Table I but the energy resolution was mostly limited by the leakage current of the detector or by the noise of the FEE. Till few years ago, the best published result at room temperature is 260 eV FWHM at +25°C at 5.9 keV (^{55}Fe) for a 25 mm^2 SDD [9], which is anyhow well far away from the resolution of 123-125 eV FWHM obtained with peltier-cooled SDDs [15, 16, 17]. Last year, the first achievements of the research activity of our group in designing SDDs and FEE with ultimate low noise was presented [8], demonstrating for the first time the capability for a SDD-CMOS FEE system to operate up to room temperature with the highest energy resolution (141 eV FWHM) possible so far, approaching the value achievable with cooled devices. In this paper, we present improved and extended experimental results of the SDD-CMOS FEE system together with their detailed analysis: in Section II the detector design, fabrication and electrical characterization are presented; Section III is devoted to the Front-End Electronics and Section IV to the System characterization; an analysis of the system's noise is presented in Section V.

TABLE I
X-RAY SDD PERFORMANCE AT ROOM TEMPERATURE

Reference	year	Detector area (mm^2)	Temperature (ºC)	5.9 keV ^{55}Fe FWHM (eV)	ENC (e- r.m.s.)	Peaking time (µs)
This work	2015	13	+20	136	7.4	1.4
[8]	2014	13	+21	141	8.6	0.8
[9]	2012	25	+25	260	27	0.1
[10]	2001	10	+25	300	--	--
[11]	1996	3.5	+27	220	21	0.5
[12]	1994	2	+24	(374)	41	--
[13]	1994	1.5	+20	327	--	7
[13]	1994	0.5	+20	267	--	7
[14]	1992	78	R.T.	940	110	0.25

II. THE SILICON DRIFT DETECTOR

A. Fabrication technology

The detector was realized on a <100> floating zone silicon wafer, n-type, 150 mm diameter, 450 µm thick.

The fabricated SDD is hexagonal with an active area of 13 mm^2 and the anode in the center. A continuous p+ cathode constitutes the entrance window on one side of the detector. The cathodes on the anode-side are biased through an integrated resistive voltage divider in order to create the drift field. The hexagonal structure is functional to a matrix configuration [18]. An innovative and proprietary technological process (LC-SDD/Low Current SDD) – driven also by the need of very large area SDDs [19] - has been developed at FBK to reduce the reverse currents of the pn junctions in order to minimize the dark current at the anode.

B. Electrical characterization

The SDD has been glued on the printed circuit board together with the Charge Sensitive Preamplifier (CSA, described in Section III), placed in thermostatic chamber

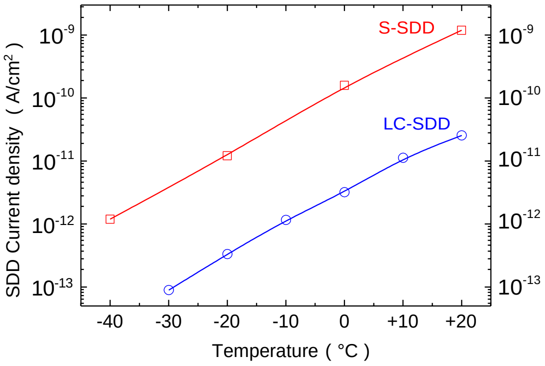

Figure 2 Current densities measured at the anode of two Silicon Drift Detectors in operative conditions as function of the temperature. The SDD fabricated with the new Low Current process (LC-SDD) shows an anode current about 50 times lower than the SDD fabricated with standard process (S-SDD).

and biased at the operating conditions and firstly checked with a radioactive source. The anode current (I_{anode}) has been measured as a function of the temperature. Since the CSA operates in pulsed-reset mode, the anode current is periodically integrated into the feedback capacitance, so that I_{anode} can be determined from the slope of the CSA output voltage. The feedback capacitance has been accurately measured from the amplitude of the signals generated by the 5.9 keV line of a ^{55}Fe radioactive source. The results of the measurements are shown in Figure 2 in terms of current density. The same figure also shows the current density measured on a similar SDD fabricated with a standard process (S-SDD). At a temperature T = +20°C the current density of the LC-SDD is J=25 pA/cm^2 while it is J=1.2 nA/cm^2 for the S-SDD showing a significant reduction by a factor 48 achieved with the LC-process. The slope of the two I-T curves are approximately the same and so almost the same reduction factor is also observed at all the other temperatures. At T = -30°C the measured current densities are J=4 pA/cm^2 and J=90 fA/cm^2 for the standard and LC process, respectively.

It can be observed that the S-SDD must be cooled down to T= -14°C in order to reach the same anode current the LC-SDD shows at T=+20°C, so the new technology allows to gain ΔT=+34°C in terms of operating temperature to have the same detector noise. Considering that the lowest anode current density of SDDs declared so far is 200 pA/cm^2 at room temperature [17], this technology sets the new state of the art improving by an order of magnitude. Since the parallel noise *ENC* contribution depends on the root square of the anode current, a significant improvement by a factor 3 in this noise component is expected.

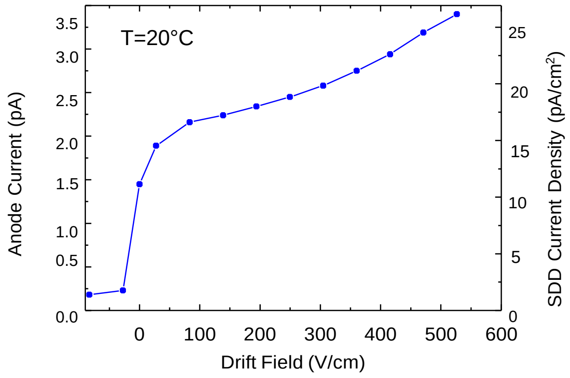

Figure 3 Anode current of LC-SDD and current density (right y-axis) measured at +20°C as function of the drift field.

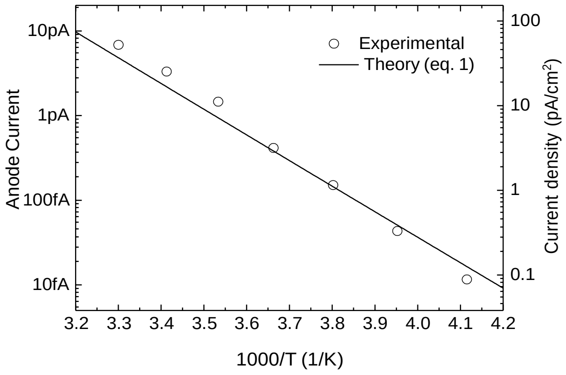

Figure 4. Anode current vs. 1000/T. An acceptable agreement with the theoretical generation current (eq. 1) is found, deriving a carrier effective lifetime of τ_o=1.16 s.

Figure 3 shows the anode current measured at T=+20°C as a function of the drift field, which has been changed by setting the outmost drift cathode bias voltage while keeping both the first and the entrance window cathodes bias voltages constant. An increase of the current density from 17 to 25 pA/cm^2 as the drift field is changed from 100 to 500 V/cm is measured. Such a growth can be explained with the increasing of the generation current due to the widening of the depleted inter-cathode surfaces and/or due to the increasing of the charge generation rate in the regions in close proximity to the voltage divider, where a local rising of the temperature is expected due to the increment of the electrical power in the integrated resistors.

Assuming that the anode current is dominated by thermal generation of charge carriers in the depleted silicon, we can write [20, 21]

$$I_{anode} = AW\frac{n_i}{2c_o} = \frac{AW}{2c_o}\sqrt{N_{Co}N_{Vo}}\left(\frac{T}{T_o}\right)^{3/2} e^{-\frac{E_g}{2kT}} \qquad (1)$$

in which *A* and *W* are the area and the thickness of the depleted region, respectively; n_i is the intrinsic carrier concentration, τ_o is the effective carrier lifetime, N_{Co}=2.86x10^{19} cm^{-3} and N_{Vo} =3.1x10^{19} cm^{-3} are the effective density of states in the conduction and valence bands, respectively at the reference temperature T_o=300 K [22]; E_g, *k* and *T* are the bandgap energy, the Boltzmann constant and the absolute temperature. The experimental data have been fitted to eq. 1 as shown in Figure 4 finding an acceptable agreement, in a first approximation. The carrier effective lifetime derived from the fitting is τ_o = 1.16 s, which reveals a significant improvement with respect the value of 15 ms originally measured by J. Kemmer et collaborators in 1982 with the first silicon detector based on *pn* junctions made using planar technology [23].

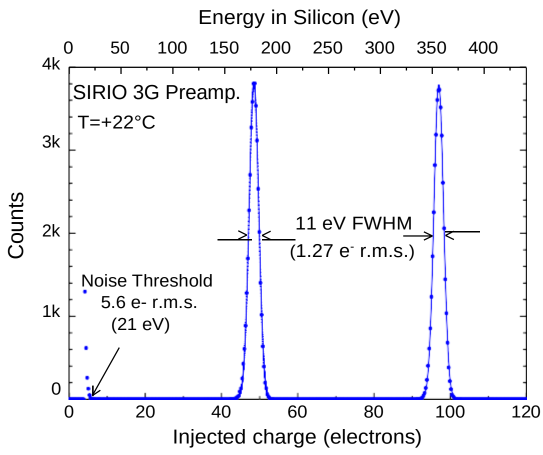

Figure 5. Artificial spectrum acquired at +22°C before connecting the preamplifier input to the detector anode. The measured ENC of 1.27 e- r.m.s. (11 eV FWHM) represents the system noise, disturbances and interference included, but without the detector contribution. The noise threshold is at only 5.6 electrons (21 eV).

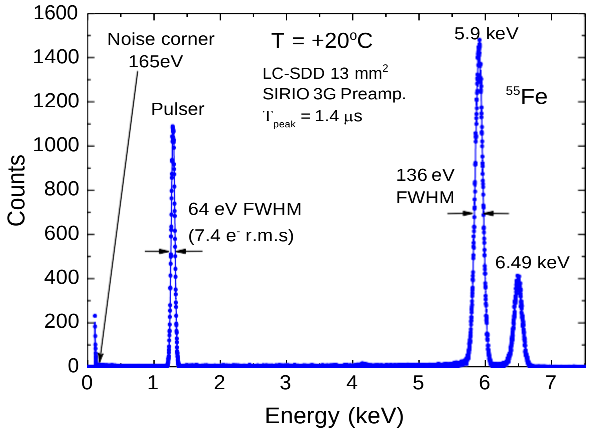

Figure 6 ^{55}Fe acquired at +20°C amd optimum peaking time (1.4 µs). The pulser line width is 64 eV FWHM, corresponding to 7.4 electrons r.m.s..

III. THE SIRIO PREAMPLIFIER

The front-end electronics of our system is constituted by an ultra low-noise CMOS Charge Sensitive Preamplifier (CSA) named SIRIO, which is the result of several years of research activity focused to achieve the lowest noise in CMOS CSA. Its first version, designed for SiC pixel detectors, demonstrated an *ENC*=3.9 electrons r.m.s. at room temperature [6]. In this experiment we used the third generation of such CSAs (SIRIO-3G), which has an intrinsic Equivalent Noise Charge (ENC) around 1.3 electron r.m.s. at room temperature and even lower than 1 electron r.m.s. at -30°C [24]. A SIRIO-3G chip has been glued onto the detector in close proximity to the anode in order to minimize the bonding wire length and so the associated stray capacitance.

IV. EXPERIMENTAL

A. Experimental setup

The detector-preamplifier system was placed inside a metal box in a thermostatic chamber. The system was operating in dry air, obtained by fluxing N_2 and by hygroscopic salts, the temperature was constantly measured by a thermocouple. A precision pulser (Tektronix AFG3022B) was used to inject calibrated charge pulses through the test capacitance (C_{TEST}) integrated in the CSA in order to directly measure the electronic noise of the system. The preamplifier output signal have been processed by a digital pulse processor (Amptek PX5) implementing a triangular shaping with peaking times settable from 0.4 µs to 102 µs.

B. Readout Electronics characterization

The readout electronics has been tested before connecting the detector anode to the preamplifier input in order to measure the noise of the system without the detector contribution. The Equivalent Noise Charge (ENC) has been measured acquiring artificial spectra by injecting a sequence of two calibrated charge pulses by means of the pulser. The injected charge has been first estimated by considering the nominal value of C_{TEST} and then accurately determined when the detector was connected, by measuring C_{TEST} using a ^{55}Fe spectrum. Figure 5 shows the spectrum acquired at T=+22°C by injecting two sets of charge pulses of about 50 and 100 electrons, equivalent to about 183 eV and 367 eV deposited in Silicon. At the optimum peaking time of 51 µs a minimum FWHM of 11 eV has been measured, corresponding to ENC= 1.27 electrons r.m.s. The threshold of the noise is at only 5.6 electrons, corresponding to an energy of 21 eV. The *ENC* was measured also at T=-30°C, resulting in a minimum noise of 1.0 electrons r.m.s. (8.7 eV FWHM). The *ENC* of the system versus the peaking time at T=+22°C and T=-30°C before connecting the detector is shown in Figure 9, indicated for simplicity as “SIRIO preamplifier” although it represents the system noise, disturbances and interference included, excluding only the contribution of the detector and of the preamplifier-detector connection wire to the system noise.

C. System characterization with X-rays

After connecting the anode at the preamplifier input by wire bonding, the SDD-SIRIO system has been characterized with the ^{55}Fe and the pulser lines. No photon collimation was used during irradiation. Figure 6 shows the best spectrum of ^{55}Fe acquired at room temperature (T=+20°C) with a peaking time of 1.4 µs. The width of the 5.9 keV line is 136 eV FWHM, the pulser line width is 64 eV FWHM, corresponding to 7.4 electrons r.m.s.. The noise threshold is at 165 eV (45 electrons). To our best knowledge, this is the highest energy resolution ever measured with a semiconductor detector of such area (13 mm^2) and operated at room temperature. Comparing this result with previously published value for 5.9 keV FWHM reported in Table I, the significant progress can be appreciated.

The system was also tested at different temperatures from T=+30°C down to T=-30°C. Figure 9 shows the pulser line FWHM and the corresponding *ENC* as a function of the peaking time at the different operating temperatures and Table II reports the minimum line width measured at each

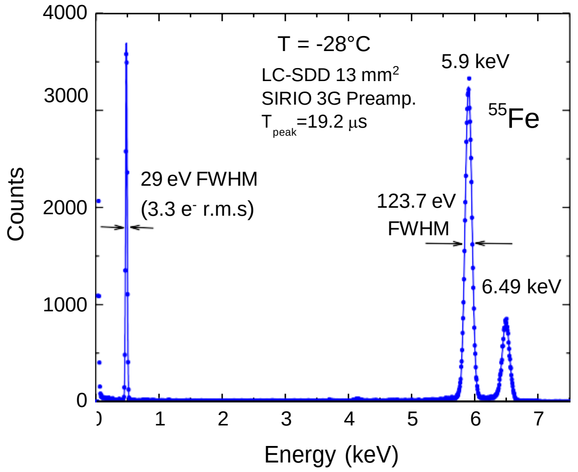

Figure 7. ^{55}Fe acquired at -28°C and optimum peaking time (19.2 µs).. The pulser line width is 29 eV FWHM, corresponding to 3.3 electrons r.m.s..

temperature and the corresponding peaking time. The system noise at the optimum peaking times, ranges from 82 eV FWHM at T=+30°C down to 29 eV FWHM at T=-30°C. The ^{55}Fe spectrum acquired at T=-28 °C is shown in Figure 7: the width of the 5.9 keV line is 123.7 eV FWHM and the pulser line width is 29 eV FWHM, equivalent to 3.3 electrons r.m.s. at a peaking time of 19.2 µs. The peak to valley ratio in the ^{55}Fe spectrum was not high (≈10^3) because of the absence of a photon collimator, so that the FWHM can be probably improved even further with the use of a well-designed collimator.

V. SYSTEM NOISE ANALYSIS

A. *Introduction*

In this section an analysis of the measured noise is presented allowing to derive some significant information on the system. Specifically, this analysis aims to determine the noise contributions of the detector and of the readout electronics, finding the limiting factor to the performance of the system in terms of energy resolution. Moreover, a fitting of the experimental *ENC vs.* T_{peak} data will give the weight of the different noise components and the effect of the stray capacitances due to the bonding connection.

TABLE II
LC-SDD-SIRIO: SYSTEM ENERGY RESOLUTION AND NOISE

T [°C]	^{55}Fe 5.9 keV LINE WIDTH [eV FWHM]	PULSER LINE WIDTH [eV FWHM]	ENC [e- r.m.s.]	Peaking Time (µs)
+30	148	82	9.4	0.8
+20	136	64	7.4	1.4
+10	133	53	6.1	2.4
0	129	44	5.0	4.8
-10	129	41	4.7	9.6
-30	123.7	29	3.3	19.2
READOUT ELECTRONICS				
+22	--	11	1.27	51.2
-30	--	8.7	1.0	102.4

B. *Noise components analysis*

The analysis of the system noise has been done by considering the classical model for the Equivalent Noise Charge:

$$ENC_{tot} = \sqrt{ENC_{ws}^2 + ENC_{1/f}^2 + ENC_{wp}^2} \qquad (2)$$

in which the total noise is given by the white series (*ws*), *1/f* and white parallel (*wp*) components, whose detailed expressions can be found in [25]. Figure 8 shows the fitting to Eq. 2 of the experimental *ENC* vs. T_{peak} data taken at T=+20°C. The model well describes the experimental data allowing to precisely disentangle the three noise components. From the white series noise a total input capacitance of about 130 fF can be derived, from the white parallel component a leakage current of 3.8 pA is calculated, in good agreement with the value measured from the slope of the preamplifier output; the *1/f* component is contributing for about 4.8 electrons, which is almost the same value given by the series and parallel noise at the optimum peaking time of 1.2 µs.

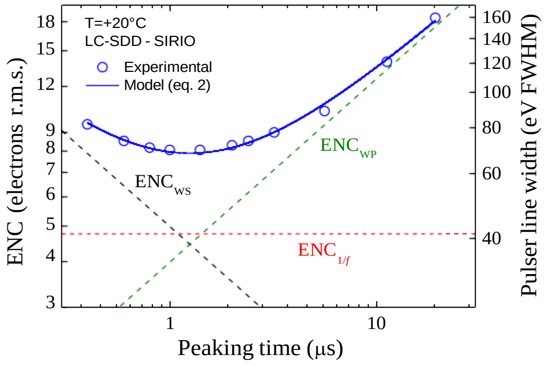

Figure 8 LD-SDD+SIRIO system at room temperature (+20°C): Equivalent Noise Charge (left y-axis) and corresponding pulser line width (right y- axis) versus peaking time. The main noise components are derived by fitting the experimental data to equation 2.

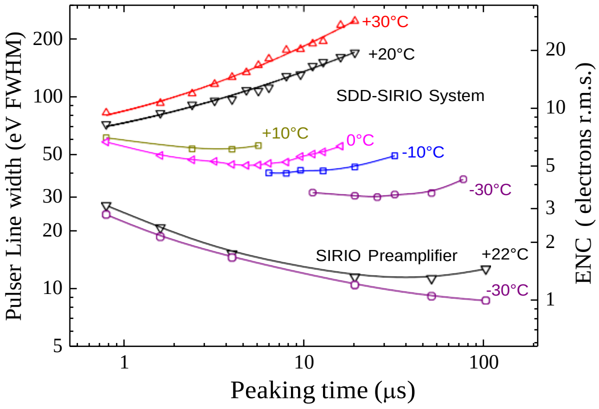

Figure 9 Pulser line width and *ENC* for the whole System and of the SIRIO preamplifier alone, measured at different temperatures as function of the peaking time of a triangular pulse shaping.

C. Discussion on Detector and Front-End noise contributions

The noise of the system has been measured before and after connecting the detector anode to the preamplifier input. The results have been reported in Figure 9: the *ENC* measured before the connection of the detector ranges from 3 e$^-$ r.m.s. (26 eV FWHM) at T=+22 °C and T_{peak}=0.8 µs down to 1.0 e r.m.s. (8.7 eV FWHM) at T=-30 °C and T_{peak}=102 µs. Such noise includes mainly the preamplifier intrinsic noise (so the curves have been indicated as SIRIO preamplifier) but also any noise component injected from the power supplies and any disturbance coming from the surrounding environment. Comparing the noise measured before and after connecting the detector, it is clear that, at all the temperatures, the connection of the detector brings to a significant increase of the system noise because of the relevant growth of both the parallel and series noises due to the detector anode current and to the detector and wire bonding capacitances, respectively. This becomes even more evident if we consider that the *ENC* contributions sum quadratically: at T=-30°C, for example, *ENC* grows from 0.9 to 3.3 electrons r.m.s., that is a variation of an order of magnitude; this increase is due to several effects. As far as the parallel noise is concerned, the preamplifier is practically noiseless at all the temperatures, since the leakage current at its input ranges from 1 fA at T=+20°C down to few aA at T=-30°C, so that the whole parallel noise of the system comes from the detector. The series noises (white and *1/f*) have their origin in the preamplifier (mainly from the input transistor), but their intensities in the final system are strongly determined by the capacitance of the detector (C_D) and of the wire connection (C_w). In Figure 9, the significant increase of both the series noise components when the detector is connected can be appreciated but, in an ideal case of C_D+C_w=0, we wouldn’t observe any increase in these noise components. From these considerations on noise components we can conclude that the detector - even if it presently represents the state of the art - and the preamplifier/detector wire connection, are significantly determining the system energy resolution at all temperatures. At the same time, in principle, also the preamplifier design can be further improved to reduce the *ENC* sensitivity to the to the input load capacitance.

VI. CONCLUSIONS

We have designed and experimentally characterized an X-ray spectroscopic system constituted by a Silicon Drift Detector and a CMOS integrated preamplifier (SIRIO) demonstrating that very high energy resolution – with pulser linewidth equal or less than 82 eV FWHM - can be obtained even with the system operating at room temperature. This results have been made possible by two parallel and concurrent research activities: the first was related to an improved detector manufacturing technology which allowed to decrease the reverse current density of the pn junctions at ultra-low levels (anode current density lower than <25 pA/cm^2 at room temperature); the second was an advanced design of a CMOS charge sensitive preamplifier showing an intrinsic noise close to 1 electron r.m.s. at room temperature.

The energy resolution measured at +20°C (136 eV FWHM at 5.9 keV from ^{55}Fe) is not so far from that one (124 eV FWHM) achieved with state of the art system cooled between -20°C and -50°C using Peltier cooling systems. Besides, the measured energy resolution is the highest ever achieved at room temperature by any semiconductor detector of comparable active area opening new perspectives in the technological implementation and applications of these types of X-ray spectrometers.

ACKNOWLEDGMENT

This research has been supported by Politecnico di Milano, the National Institute of Nuclear Physics (INFN) and Fondazione Bruno Kessler (FBK). Authors thanks S. Masci for system assembly and wire bondings, A.C. Huber and R.H. Redus for the optimized digital pulse processor used in these experiments.

REFERENCES

---

1 E. Gatti, P. Rehak, “The Concept of A Solid State Drift Chamber”, Proceedings of The 1983 DPF Workshop on Collider Detectors: Present Capabilities and Future Possibilities, Feb. 28 - March 4, 1983, Lawrence Berkeley Laboratory, University of California, Berkeley, California 94720

2 E. Gatti, P. Rehak, “Semiconductor drift chamber — An application of a novel charge transport scheme”, Nuclear Instruments and Methods in Physics Research, Volume 225, Issue 3, 1 September 1984, Pages 608-614

3 E. Gatti, P. Rehak, “Review of semiconductor drift detectors”, Nuclear Instruments and Methods in Physics Research A 541 (2005) 47–60

4 Chiara Guazzoni, “The first 25 years of silicon drift detectors: A personal view”, Nuclear InstrumentsandMethodsinPhysicsResearchA624(2010)247–254.

5 O'Connor, P. ; Gramegna, G. ; Rehak, P. ; Corsi, F. ; Marzocca, C., “CMOS preamplifier with high linearity and ultra low noise for X-ray spectroscopy”, IEEE Transactions on Nuclear Science, Volume: 44 , Issue: 3 , Part: 1 DOI: 10.1109/23.603663, 1997, Page(s): 318 - 325

6 G. Bertuccio, S. Caccia, ”Progress in ultra-low-noise ASICs for radiation detectors”, Nuclear Instruments and Methods in Physics Research, A Volume: 579, Issue: 1, August 21, 2007, pp. 243-246

7 Bombelli, L. ; Fiorini, C. ; Frizzi, T. ; Alberti, R. ; Longoni, A., “CUBE, A low-noise CMOS preamplifier as alternative to JFET front-end for high-count rate spectroscopy”, Proceedings of the 2011 IEEE Nuclear Science Symposium and Medical Imaging Conference (NSS/MIC), DOI: 10.1109/NSSMIC.2011.6154396, 2011, pp. 1972-1975

[8] G. Bertuccio, M. Ahangarianabhari, C. Graziani, D. Macera, Y. Shi, A. Rachevski, I. Rashevskaya, A. Vacchi, G. Zampa, N. Zampa, P. Bellutti, G. Giacomini, A. Picciotto and C. Piemonte, “A Silicon Drift Detector-CMOS front-end system for high resolution X-ray spectroscopy up to room temperature” Journal of Instrumentation, vol 10, January 2015 (IWORID 2014 – Trieste) 2015 1748-0221 10 P01002

9 L. Bombelli, C. Fiorini, T. Frizzi, R. Alberti, R. Quaglia, “High rate X-Ray spectroscopy with "CUBE" preamplifier coupled with Silicon Drift Detector” 2012 IEEE Nuclear Science Symposium and Medical Imaging Conference Record (NSS/MIC) Nl-202

10 P. Lechner, C. Fiorini, R. Hartmann, J. Kemmer, N. Krause, P. Leutenegger, A. Longoni, H. Soltau, D. Stotter, R. Stotter, L. Struder, U. Weber, “Silicon drift detectors for high count rate X-ray spectroscopy at room temperature”, Nuclear Instruments and Methods in Physics Research A 458 (2001), 281-287

11 Peter Lechner, Stefan Eckbauer, Robert Hartmann, Susanne Krisch, Dieter Hauff, Rainer Richter, Heike Soltau, Lothar Strüder, Carlo Fiorini, Emilio Gatti, Antonio Longoni, Marco Sampietro, “Silicon drift detectors for high resolution room temperature X-ray spectroscopy”, Nuclear Instruments and Methods in Physics Research Section A, Vol. 377, Issues 2–3, 1 August 1996, Pages 346-351.

12 R.Hartmann, D.Hauff, S.Krisch, P.Lechner, G.Lutz, R.H.Richter, H.Seitz, L.Struder, G.Bertuccio, L.Fasoli, C.Fiorini, E.Gatti, A.Longoni, E.Pinotti, M.Sampietro, "Design and test at room temperature of the first Silicon Drift Detector with on chip electronics" IEEE International Electron Devices Meeting, San Francisco (CA), USA, Dec.11-14, 1994. IEDM 94 Technical Digest pp.535-538 - IEEE Catalog Number 94CH35706, IEEE, Piscataway, NJ 08855 (USA), 1994.

13 Jalas, P. ; Niemela, A. ; Chen, W. ; Rehak, P. ; Castoldi, A. ; Longoni, A., “New results with semiconductor drift chambers for X-ray spectroscopy”, IEEE Transactions on Nuclear Science, Vol. 41, Issue 4 , DOI: 10.1109/23.322856, 1994 , pp. 1048-1053.

14 G. Bertuccio, M. Sampietro, A. Fazzi, "High Resolution X-ray Spectroscopy with Silicon Drift Detectors and Integrated Electronics", Nucl. Instr. Meth., A322, (1992), 538-542.

15 R. Quaglia, L. Bombelli, C. Fiorini, M. Occhipinti, P. Busca, G. Giacomini, F. Ficorella, A. Picciotto, C. Piemonte, “New Developments of SDD-based X-ray Detectors for the Siddharta-2 Experiment” , Proceeding of the Nuclear Science Symposium and Medical Imaging Conference (NSS/MIC), 2013 IEEE.

16 R. Redus, A. Huber, J. Pantazis, T. Pantazis, “Enhanced Energy Range Thermoelectrically Cooled Silicon X-ray Detectors”, 2011 IEEE Nuclear Science Symposium Conference Record, N13-5.

17 D.M. Schlosser, P.Lechner, G.Lutz, A.Niculae, H.Soltau, L.Struder, R.Eckhardt, K.Hermenau, G. Schaller, F.Schopper, O.Jaritschin, A.Liebel, A.Simsek, C.Fiorini, A.Longoni, “Expanding the detection efficiency of silicon drift detectors”, Nuclear Instruments and Methods in Physics Research A624(2010), 270–276.

18 A. Rachevski, G. Zampa, N. Zampa, I. Rashevskaya, A. Vacchi, G. Giacomini, A. Picciotto, A. Cicuttin, M. L. Crespo, C. Tuniz, “X-ray spectroscopic performance of a matrix of silicon drift diodes”, Nuclear Instruments and Methods in Physics Research A718 (2013) 353–355.

19 A. Rachevski, G. Zampa, N. Zampa, R. Campana, Y. Evangelista, G. Giacomini, A. Picciotto, P. Bellutti, M. Feroci, C. Labanti, C. Piemonte and A. Vacchi, “Large-area linear Silicon Drift Detector design for X-ray experiments”, Journal of Instrumentation, vol. 9. 2014, P07014 doi:10.1088/1748-0221/9/07/P07014

20 A. S. Grove, “Physics and Technology of Semiconductor devices”, 1967, John Wiley & Sons, Inc., New York, USA.

21 S.M. Sze, “Physics of Semiconductor Devices”, 2nd edition, 1981, John Wiley & Sons, Inc., pp. 19 and 91.

22 M. A. Green, “Intrinsic concentration, effective densities of states, and effective mass in silicon”, Journal of Applied Physics 67, 2944 (1990), pp 2944-2954.

23 Kemmer, J. ; Burger, P. ; Henck, R. ; Heijne, E., “ Performance and Applications of Passivated Ion-Implanted Silicon Detectors”, IEEE Transactions on Nuclear Science, Vol. 29 , Issue 1, 1982 , pp. 733 - 737

24 G. Bertuccio, D. Macera, C. Graziani, M. Ahangarianabhari
“A CMOS Charge Sensitive Amplifier with sub-electron Equivalent Noise Charge”, To be published on the Proceedings of the 2014 IEEE Nuclear Science Symposium, Seattle – WA - USA, 8-15 Nov. 2014.

25 G. Bertuccio, S. Caccia, ” Noise Minimization of MOSFET Input Charge Amplifiers based on $\Delta\mu$ and ΔN $1/f$ Models”, IEEE Transactions on Nuclear Science, Vol. 56, no. 3, 2009, pp. 1511 – 1520